

Article

Transmission Capacity Characterization in VANETs with Enhanced Distributed Channel Access

Wei Liu ¹, Xinxin He ², Zhitong Huang ¹ and Yuefeng Ji ^{1,*}

¹ State Key Lab of Information Photonics and Optical Communications, Beijing University of Posts and Telecommunications, Beijing 100876, China; lw_9000@bupt.edu.cn (W.L.); hzt@bupt.edu.cn (Z.H.)

² Beijing Key Laboratory of Network System Architecture and Convergence, Beijing University of Posts and Telecommunications, Beijing 100876, China; hxx_9000@bupt.edu.cn

* Correspondence: jyf@bupt.edu.cn

Received: 14 January 2019; Accepted: 15 March 2019; Published: 20 March 2019



Abstract: The traditional research on the capacity of the Vehicular Ad Hoc Networks (VANETs) mainly lacks realistic models mimicking the behaviors of vehicles and the MAC protocol applied by IEEE 802.11p. To overcome these drawbacks, in this paper, the network transmission capacity analysis for VANETs is carried out from the perspective of the spatial geometric relationship among different vehicles. Specifically, the transmission scheme in this system is set to mimic enhanced distributed channel access (EDCA) protocol, in which the division of priorities is taken into account both the data type and the transmission distance requirement. Meanwhile, the moving pattern of vehicles is described as the classic car-following model according to realistic characteristics of VANET, and the propagation channel is modeled as a combination of large-scale path-loss and small-scale Rayleigh fading. Based on this model, the transmission opportunity under EDCA protocol is quantified and compared with that of CSMA/CA, and then the outage probability is calculated under the worst interfered scenario. Finally, the transmission capacity is thereby calculated and verified by the simulation results.

Keywords: VANET; Transmission Capacity; EDCA; Car-following

1. Introduction

Vehicular ad-hoc networks (VANETs) have attracted significant interests in industries and the academia in recent years [1,2]. To support various applications, the Federal Communications Commission (FCC) allocated 75 MHz in 5.9 GHz band for dedicated short-range communication (DSRC) [3]. The applications in VANETs deliver functions and services mainly in traffic safety and consumer convenience [4,5]. With the rapid development of traffic, the frequent use of the aforementioned applications for communication continues to increase, however, the network capacity of VANET is limited and the transmission QoS is difficult to be guaranteed. Therefore, the network capacity analysis of VANET is still necessary.

Gupta and Kumar [6] initially developed the concept and expression of transport capacity in wireless ad hoc networks following the scaling-law based analysis method. They proved that a sum network capacity $\Omega(\sqrt{n/\log n})$ is feasible in a generic ad hoc network with n nodes. The definition of transmission capacity has far-reaching significance for the study of wireless ad hoc network capacity. For the first time, the transmission distance is related to the network capacity, and it has been widely recognized by the academic community. Based on this pioneering work, a number of studies extend the theories in different transmission scheduling and routing schemes [7,8]. Generally, most of these existing researchers only characterize the capacity performance changing pattern by scaling laws, and these results cannot directly estimate the actual capacity of the entire network with some specific

parameters are given. Therefore, some scholars consider using stochastic geometry tools [9,10] to model wireless ad hoc networks. The received signal-to-interference-noise ratio (SINR) of the transmission channel in the network is calculated by stochastic geometry theory, and then the transmission outage probability and network capacity are measured. Among them, the popular definition of wireless ad hoc network capacity is transmission capacity. In Reference [11], the definition of transmission capacity is proposed by S. Weber and J. G. Andrews based on the concept of transport capacity in Reference [6]. The transmission capacity is described as the maximum number of bits transmitted by all nodes in a unit area per unit time under the constraints of a given outage probability, which gives a quantitative analysis of the influence of network node density and channel fading on network capacity. However, the nodes in Reference [11] are usually randomly scattered on a 2-dimensional plane, which cannot directly represent the actual distribution of vehicles on a straight highway. On the other hand, the MAC layer protocols analyzed in Reference [11] are not capable of realistically modeling enhanced distributed channel access (EDCA) equipped by IEEE 802.11p standard-based VANET.

In this paper, we study the transmission capacity of a 1-dimensional VANET under EDCA protocol. In Reference [11], the transmission capacity in this paper is defined as the average expected spatial density of successful transmissions in the network. To make more realistic conclusions, the Car-following Model is utilized to incorporate the impact of vehicle mobility on the network capacity, and Rayleigh fading environment effect is considered during the computing of transmission outage probability. Our theoretical results can provide a theoretical reference for the development of MAC layer access protocols and standards in the field of Internet of VANETs. Additionally, the network performance of the new protocol can be analyzed by using our theoretical model. In consequence, there are three main contributions of this paper.

- The transmission scheme is modeled to mimic EDCA protocol from the perspective of the spatial geometric relationship among transmitters, in which the division of priorities takes into account both the data type and the transmission distance requirement. and the transmission opportunity under EDCA protocol is calculated and compared with that of CSMA/CA.
- More realistic characteristics of the VANET are considered, for instance, the moving pattern of vehicles is described as the classic car-following model, and the propagation channel is modeled as the combination of path-loss and Rayleigh fading.
- With the theoretical results obtained from the analysis on spatial transmission opportunity and outage probability, the network transmission capacity of VANETs is thereby calculated and also verified by simulations.

The rest paper is organized as follows: In Section 2, the related works are summarized, and the system model of 1-dimensional VANET is introduced in Section 3. In Section 4, the transmission scheme is theoretically modeled, and transmission capacity under Rayleigh fading channels is analyzed. Simulation results are illustrated in Section 5. Finally, the paper is concluded in Section 6.

2. Related Works

While the research on network capacity in the traditional wireless ad hoc network has achieved outstanding results, the existing results cannot be directly applied to the vehicular field due to some basic characteristics of VANET. In VANET, vehicle nodes move along the road with regular constraints and can be statistically distributed according to road conditions, and the EDCA protocol is adopted in MAC layer. Some new protocols have designed and proposed for traffic safety data dissemination. In Reference [12], inter vehicle distance is analyzed within connectivity aware routing design for data dissemination. Additionally, in Reference [13], a channel selection framework for location-oriented services in VANET is proposed. However, the performance evaluation of these protocols does not take into account network capacity.

Recently some researchers have focused on VANET capacity analysis. Considering that the transmission range of vehicles is much larger than the width of roads, network topology is usually

modeled as a one-dimensional linear or urban grid model. In References [14,15], the urban traffic network model is described as an extended grid model, and the network asymptotic throughput performance is analyzed intuitively based on protocol model by scaling laws without considering the influence of vehicle distribution and channel fading. Reference [16] analyzed the asymptotic throughput scaling based on physical model without considering the small-scale channel fading. Some studies are present based on a one-dimensional linear model. In References [17–19], the authors investigated the maximum density of successful simultaneous transmitters in VANETs, but did not take the interference into account in the transmission. In References [20–24], the authors proposed the estimation of network capacity in VANETs by considering the impacts of interference. However, in these studies, all data-packets are assumed to hold the same priority, and the task of modeling EDCA is simplified as carrier sense multiple access with collision avoidance (CSMA/CA) which cannot really evaluate the performance of the network. In Reference [25], we have proposed transmission capacity analysis for VANET integrally considering the impacts of the CSMA/CA mechanism, channel fading, and vehicle distribution, however, the MAC protocol is also simplified. In Reference [26], a priority based MAC is proposed to support the non-safety applications in V2I communication. In this paper, the priority based transmission scheme in MAC layer is designed and analyzed by taking into account both the data type and the transmission distance requirement. Meanwhile, more realistic characteristics of the VANET are considered during the transmission capacity calculation, for instance, the moving pattern of vehicles is described as the classic car-following model, and the propagation channel is modeled as the combination of path-loss and Rayleigh fading.

3. System Model

In this section, the system model is divided into 1-dimensional VANET model and slotted medium access protocol model for analysis, and performance metrics are proposed at last. The many symbols used in this section and later have been summarized in Table 1.

Table 1. Summary of Notations.

R	Transmitting data-rate of the vehicle
P_t	Transmitting power of the vehicle
P_r	The received power of the vehicle
d_s	Propagation distance between the transmitter and the receiver
α	Path-loss exponent
H	Rayleigh fading factor
θ_d	The threshold of the transmission range between the transmitter and the receiver
Q	The total transmission opportunity under EDCA protocol
Q_q	The probability that a vehicle is preselected
Q_c	The probability that the preselected vehicle successfully transmits
C_T	Transmission capacity
λ	The density of the potential transmitters
θ_c	The CCA threshold in sensing period
θ_q	Predefined carrier sensing threshold in the contention period
λ_t	The density of the active transmitters which occupied the channel at the same time
λ_q	The density of the eligible transmitters after the sensing period
T	The backoff time
t	The total time that the eligible vehicle in the contention period needs to wait
τ	Outage probability
β	The threshold of SIR

3.1. 1-Dimensional VANET Model

The VANET model is shown in Figure 1. Since the length of the road and the radio maximal effective transmission radius are much larger than the road width, the highway is theoretically modeled as a 1-dimensional line, and the signal coverage of one transmitter is illustrated as a 2D-length segment with the transmitter at the midpoint, where D is the maximal effective transmission radius about 500 meters. In the case of sparse node density, the broadcast transmission between the transmitter and neighboring receivers can be approximately modeled as several parallel transmission pairs. For ease of calculation and analysis, we assume that a transmitting node only pairs one receiving node. The distribution of vehicles is assumed as the classic car-following model, in which the distance X between neighbors follows log-normal distribution with μ and σ [27],

$$f_X(x) = \frac{1}{\sqrt{2\pi\sigma x}} \exp\left(-\frac{(\ln x - \mu)^2}{2\sigma^2}\right), \tag{1}$$

All vehicles are assumed to equip with the same transmitting data-rate R and power P_t . The propagation signal power decays with distance increases and experiences with the small-scale Rayleigh fading. Therefore, the received power is expressed as

$$P_r = P_t H d_s^{-\alpha} \tag{2}$$

where d_s denotes the propagation distance between the transmitter and the receiver, α is the path-loss exponent, H denotes the Rayleigh fading factor following exponential distribution with unit mean, that is, $f_H(x) = \exp(-x)$.

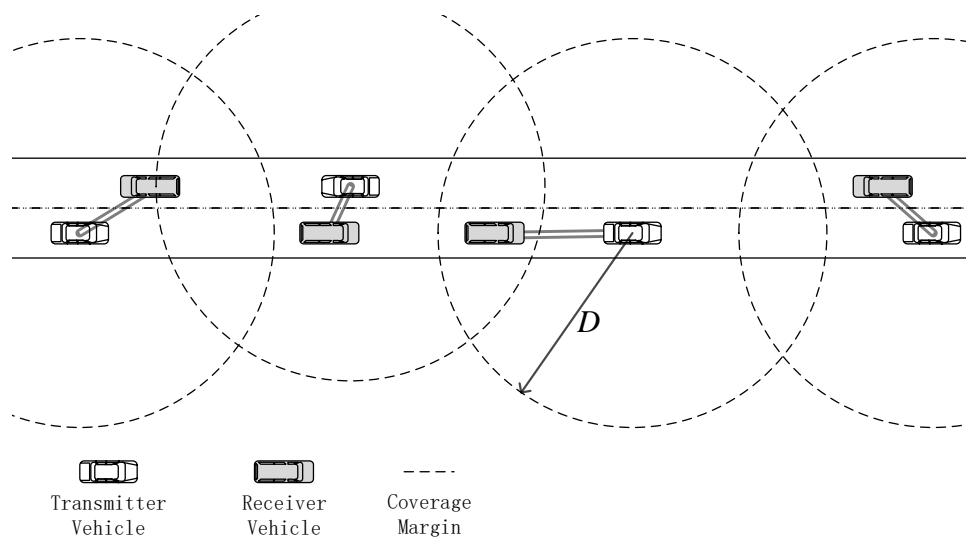


Figure 1. Basic illustration of theoretical model.

3.2. Slotted Medium Access Protocol Model

IEEE 802.11p adopts the EDCA protocol to ensure the quality of service (QoS) of different data services and achieve reasonable resource allocation [28]. EDCA divides the application messages into four access categories (ACs) according to the delay sensitivity, which are AC service access (AC_VO), video service access (AC_VI), the best effort to deliver (AC_BE), and background information access (AC_BK). For different ACs, EDCA sets different buffer queues and each queue fulfills a classical CSMA/CA mechanism with specific parameters [29]. By setting different parameters, the different priorities are divided. For example, assigning smaller Arbitration Inter-frame Space (AIFS), CW_{\min} , and CW_{\max} to high priority service categories, it has a shorter back-off time in the contention channel,

and increases the probability of a successful contention channel. Where the CW_{min} and CW_{max} are the minimum and maximum competing window sizes, respectively.

The priority in this paper is characterized and modeled by taking into account the data service types and the transmission distance levels. The transmission distance level refers to the effective transmission range between the transmitter and the receiver. When the effective transmission range is small, the transmission distance level is high, whereas when the effective transmission range is large, the transmission distance level is low. For example, the accident is more likely to occur when the distance is closer between the vehicles, hence the warning information needs to be sent with the shortest possible delay in order to avoid accidents. The vehicle can estimate the transmission distance according to the received power of the interaction information, and determine the transmission distance level is Near (N) or Far (F). N indicates that the effective transmission range between the transmitter and the receiver is less than the threshold θ_d , and F indicates that the effective transmission range between the transmitter and the receiver is greater than the threshold θ_d . According to the data service type and transmission distance level, the priority mechanism table is shown in Table 2.

Table 2. Priority mechanism table.

Priority Level	Data Type	Distance Level	CW_{min}	CW_{max}	AIFSN
P1	AC_VO	N	$(CW_{BK_{min}}+1)/16-1$	$(CW_{BK_{min}}+1)/8-1$	$(AIFS+1)/2-3$
P2	AC_VO	F	$(CW_{BK_{min}}+1)/8-1$	$(CW_{BK_{min}}+1)/4-1$	$(AIFS+1)/2-3$
P3	AC_VI	N	$(CW_{BK_{min}}+1)/4-1$	$(CW_{BK_{min}}+1)/2-1$	$(AIFS+1)/2-3$
P4	AC_VI	F	$(CW_{BK_{min}}+1)/4-1$	$(CW_{BK_{min}}+1)/2-1$	$(AIFS+1)/2-2$
P5	AC_BE	N	$(CW_{BK_{min}}+1)/2-1$	$CW_{BK_{min}}$	$(AIFS+1)/2-2$
P6	AC_BE	F	$(CW_{BK_{min}}+1)/2-1$	$CW_{BK_{min}}$	$(AIFS+1)/2-1$
P7	AC_BK	N	$CW_{BK_{min}}$	$CW_{BK_{max}}$	$(AIFS+1)/2-1$
P8	AC_BK	F	$CW_{BK_{min}}$	$CW_{BK_{max}}$	AIFS

The estimation of transmission distance level is time-sensitive in the case of vehicle movement, and varies with the relative movement speed of the vehicle and time slot interval. Therefore, it is necessary to predict the transmission distance level of the next time slot by combine the data type for judging the data priority. Here, we use the Markov model to predict the transmission distance level of the next time slot. Assuming state S_N and state S_F represent transmission distance level N and F, respectively. The two states Markov model are shown in Figure 2, where P_{NN} represents the transition probability from state S_N to state S_N , P_{NF} is the transition probability from state S_N to state S_F , P_{FN} represents the transition probability from state S_F to state S_N , and P_{FF} is the transition probability from state S_F to state S_F .

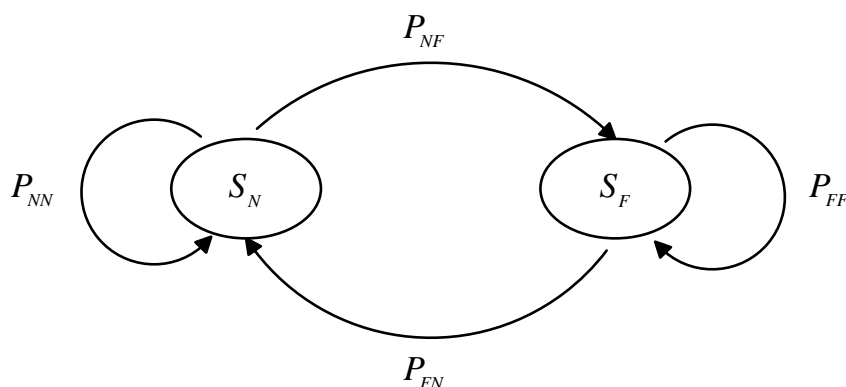


Figure 2. Two-state Markov model.

According to the definition of the transmission distance level and the state transition probability, the expressions of each state transition probability can be obtained as:

$$\begin{aligned}
 P_{FF} &= P\{S_F|S_F\} = \Pr\{d + \Delta v\Delta t > \theta_d | d > \theta_d\} \\
 P_{FN} &= P\{S_N|S_F\} = \Pr\{d + \Delta v\Delta t \leq \theta_d | d > \theta_d\} \\
 P_{NN} &= P\{S_N|S_N\} = \Pr\{d + \Delta v\Delta t \leq \theta_d | d \leq \theta_d\} \\
 P_{NF} &= P\{S_F|S_N\} = \Pr\{d + \Delta v\Delta t > \theta_d | d \leq \theta_d\}
 \end{aligned}
 \tag{3}$$

where d is the transmission distance at the current time, Δv is the relative speed between the transmitting user and the receiving user, Δt is the predicted time interval. According to the definition of conditional probability, we have

$$\begin{aligned}
 P_{FF} &= \begin{cases} \frac{\int_{\theta_d - \Delta v\Delta t}^{\infty} f_d(x) dx}{\int_{\theta_d}^{\infty} f_d(x) dx}, & \Delta v < 0 \\ 1, & \Delta v > 0 \end{cases}, & P_{FN} &= \begin{cases} \frac{\int_{\theta_d}^{\theta_d - \Delta v\Delta t} f_d(x) dx}{\int_{\theta_d}^{\infty} f_d(x) dx}, & \Delta v < 0 \\ 0, & \Delta v > 0 \end{cases}, \\
 P_{NN} &= \begin{cases} 1, & \Delta v < 0 \\ \frac{\int_0^{\theta_d - \Delta v\Delta t} f_d(x) dx}{\int_0^{\theta_d} f_d(x) dx}, & \Delta v > 0 \end{cases}, & P_{NF} &= \begin{cases} 0, & \Delta v < 0 \\ \frac{\int_{\theta_d}^{\theta_d - \Delta v\Delta t} f_d(x) dx}{\int_0^{\theta_d} f_d(x) dx}, & \Delta v > 0 \end{cases}
 \end{aligned}
 \tag{4}$$

With the probability of the current transmission distance level $P_N = \Pr\{d < \theta_d\} = \int_0^{\theta_d} f_d(x) dx$, $P_F = \Pr\{d > \theta\} = \int_{\theta_d}^{\infty} f_d(x) dx$, the probability of occurrence of state S_N and state S_F is, respectively, obtained as

$$\begin{aligned}
 FP_N &= P_N P_{NN} + P_F P_{FN} = \int_0^{\theta_d - \Delta v\Delta t} f_d(x) dx = \int_0^{\theta_d - \Delta v\Delta t} \frac{1}{\sqrt{2\pi}\beta x} e^{-\frac{(\ln x - \mu)^2}{2\sigma^2}} dx \\
 &= \frac{1}{\sqrt{2\pi}\beta} \int_0^{\theta_d - \Delta v\Delta t} \frac{1}{x} e^{-\frac{(\ln x - \mu)^2}{2\sigma^2}} dx = \sqrt{\pi} \left[1 - \exp\left\{-\frac{(\ln(\theta_d - \Delta v\Delta t) - \mu)^2}{2\sigma^2}\right\} \right]
 \end{aligned}
 \tag{5}$$

$$\begin{aligned}
 FP_F &= P_F P_{FF} + P_N P_{NF} = \int_{\theta_d}^{\infty} f_d(x) dx = \int_{\theta_d}^{\infty} \frac{1}{\sqrt{2\pi}\beta x} e^{-\frac{(\ln x - \mu)^2}{2\sigma^2}} dx \\
 &= \sqrt{\pi} \exp\left\{-\frac{(\ln(\theta_d - \Delta v\Delta t) - \mu)^2}{2\sigma^2}\right\}
 \end{aligned}
 \tag{6}$$

Therefore, the probability that the transmission distance level of the vehicle in the next time slot is grade F or grade N is calculated as follows:

$$\begin{aligned}
 P_{Next_Far} &= P\{FP_F \geq FP_N\} = P\left\{\Delta v \geq \frac{1}{\Delta t} \left[\theta_d - \exp\left(\left(\sqrt{2\ln 2} + \frac{\mu}{\sigma}\right)\sigma\right)\right]\right\} \\
 &= \frac{1}{2} - \frac{1}{2\Delta v_{\max}\Delta t} \left[\theta_d - \exp\left(\left(\sqrt{2\ln 2} + \frac{\mu}{\sigma}\right)\sigma\right)\right]
 \end{aligned}
 \tag{7}$$

$$\begin{aligned}
 P_{Next_Near} &= P\{FP_F \leq FP_N\} = P\{FP_N > FP_F\} = 1 - P_{Next_Far} \\
 &= \frac{1}{2} + \frac{1}{2\Delta v_{\max}\Delta t} \left[\theta_d - \exp\left(\left(\sqrt{2\ln 2} + \frac{\mu}{\sigma}\right)\sigma\right)\right]
 \end{aligned}
 \tag{8}$$

Assuming that the occurrence probability of each priority service type data is the same as 1/4, the priority probability in Table 1 can be calculated and obtained as

$$P_{P1} = P_{P3} = P_{P5} = P_{P7} = \frac{1}{4} P_{Next_Near}
 \tag{9}$$

$$P_{P2} = P_{P4} = P_{P6} = P_{P8} = \frac{1}{4} P_{Next_Far}
 \tag{10}$$

During the channel access process, each vehicle senses the channel before transmitting. When the channel is detected as idle, the vehicle waits for an AIFS to enter the back-off process. The value of the back-off timer is a random value in the range $[0, CW]$. The CW initial value is CW_{\min} . The value

of CW increases as a collision occurs, and remains constant when added to CW_{\max} . After the data transfer is completed, it returns to the initial value CW_{\min} . Note that the EDCA protocol customizes the maximum and minimum contention window values, and then calculates the specific values for each access type based on a certain function relationship. In the traditional distributed coordination function, the node needs to wait for a Distributed Interframe Spacing (DIFS) or Short Interframe Space (SIFS) after detecting the channel idle. In the EDCA mechanism, the DIFS and SIFS are replaced by AIFS,

$$\text{AIFS} = \text{SIFS} + \text{AIFSN} \times \text{slotTime} \quad (11)$$

where the shortest interframe interval SIFS is the same for different priority access types. Therefore, by setting the values of different AIFSNs to distinguish the frame interval of different priority services, the service with the higher priority has a shorter frame interval time.

3.3. Performance Metric

Transmission opportunity: It is defined as the probability that a node is ultimately allowed to transmit under the MAC protocol, denoted by Q .

Outage Probability (τ): It is defined as the probability that the SIR experienced by the reference receiver is below the threshold β , that is

$$\tau = \Pr\{SIR \leq \beta\}. \quad (12)$$

Transmission capacity (C_T): It is defined as the expected spatial density of successful transmissions in the networks, that is

$$C_T = \lambda Q(1 - \tau)R. \quad (13)$$

where λ is the density of the potential transmitters in the network.

4. Transmission Capacity Analysis

4.1. Subsection Transmission Opportunity Under EDCA

The EDCA can be modeled as a two-phase protocol for theoretical analysis, which includes a sensing period and a contention period. The flow chart of EDCA protocol is shown in Figure 3.

In the sensing period, each vehicle senses the channel before transmitting, and a set of vehicles are preselected only if their detecting maximum signal power is lower than the threshold θ_c . In the contention period, after querying the priority mechanism table to obtain the contention window value and arbitration inter frame space, the preselected vehicles wait for an AIFS and start the back-off process to avoid collisions among others. The value of the back-off timer is a random value in the range $[0, CW]$. The CW initial value is CW_{\min} . The value of CW increases as a collision occurs, and remains constant when added to CW_{\max} . By monitoring the medium, a pre-selected vehicle decides to start its transmission if no contender is detected to the run out of its back-off timer, otherwise it defers. That is to say, a preselected vehicle in the contention period is allowed to transmit only if it has the minimum back-off timer among all the contenders.

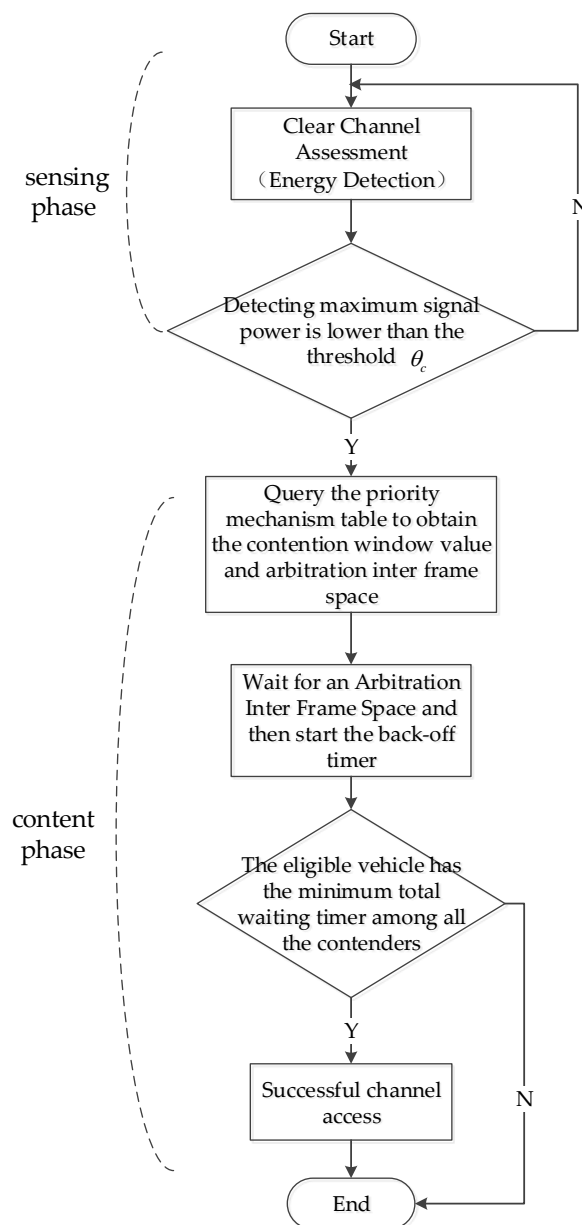


Figure 3. EDCA protocol flow chart.

The probability that a vehicle is preselected is denoted by Q_q , and the probability that the preselected one successfully transmits is denoted by Q_c . Therefore, the transmission opportunity under the EDCA protocol is expressed as $Q = Q_q Q_c$.

In the sensing period, vehicles sense the channel before transmitting at the beginning of each time slot. We first calculate the probability that a vehicle is preselected during the sensing period. Let Π_t denotes the set of active transmitters occupy the channel at the same time, and the density of Π_t is assumed as λ_t . The received signal power from the i_{th} ($i \in \Pi_t$) active transmitter occupying the channel at an arbitrary vehicle X is given by

$$S_i(x) = \frac{PH_i}{|Y_i - X|^{\alpha}}, \tag{14}$$

where Y_i is the coordinate of the i_{th} ($i \in \Pi_t$) active transmitter, and H_i is the power coefficient of the fading channel between Y_i and X . Then, the maximum received signal power at X can be denoted as

$$M(x) = \max_{i \in \Pi_t} S_i(x). \tag{15}$$

During sensing period, X is selected as an preselected transmitters only if its detecting maximum signal power is lower than the threshold θ_c , thus, Q_q can be calculated as follow:

$$Q_q = \Pr\{M(x) \leq \theta_c\}, \tag{16}$$

According to the definition of the indicating function, it can be obtained as

$$\begin{aligned} Q_q &= E[1_{\{M(x) \leq \theta_c\}}] = E\left[\prod_{i \in \Pi_p} 1_{\{S_i(x) \leq \theta_c\}}\right] = E_X\left[\prod_{i \in \Pi_p} E_h[1_{\{S_i(x) \leq \theta_c\}}]\right] \\ &= \sum_{k=1}^{\infty} \frac{(L\lambda_t^k)^k}{k!} \exp(-L\lambda_t) \left\{ \frac{1}{\sqrt{2\pi\sigma}} \int_0^{\frac{L}{2}} \frac{1}{x} \exp\left(-\frac{(\ln x - \mu)^2}{2\sigma^2}\right) P\left(H \leq \frac{\theta_c x^\alpha}{P}\right) dx \right\}^k \\ &= \exp(-L\lambda_t) \exp\left\{ \frac{L\lambda_t}{\sqrt{2\pi\sigma}} \int_0^{\frac{L}{2}} \frac{1}{x} \exp\left(-\frac{(\ln x - \mu)^2}{2\sigma^2}\right) P\left(H \leq \frac{\theta_c x^\alpha}{P}\right) dx \right\} \\ &= \exp\left\{ 2\lambda_t \int_0^{L/2} \left\{ \frac{L}{2\sqrt{2\pi}} \exp\left(-\frac{\ln^2 x}{2}\right) \left(1 - \exp\left(-\frac{\theta_c x^\alpha}{P}\right)\right) - 1 \right\} dx \right\} \\ &= \exp\left\{ L\lambda_t \left(\frac{1}{2} \operatorname{erf}\left(\frac{\ln(L/2)}{\sqrt{2}}\right) - \frac{(2\theta_c/P)^{-1/2\alpha}}{2\sqrt{2}} \operatorname{erf}\left(\left(\frac{2\theta_c}{P}\right)^{-1/2\alpha} \ln\left(\frac{L}{2}\right)\right) - 1 \right) \right\}, \end{aligned} \tag{17}$$

where (a) follows by the channel is Rayleigh faded, i.e., H is exponentially distributed with unit mean, that is $f_H(x) = \exp(-x)$.

Lemma 1. *During the sensing period in EDCA, the probability that a vehicle is selected as a preselected transmitter is given by*

$$Q_q = \exp\left\{ L\lambda_t \left(\frac{1}{2} \operatorname{erf}\left(\frac{\ln(L/2)}{\sqrt{2}}\right) - \frac{(2\theta_c/P)^{-1/2\alpha}}{2\sqrt{2}} \operatorname{erf}\left(\left(\frac{2\theta_c}{P}\right)^{-1/2\alpha} \ln\left(\frac{L}{2}\right)\right) - 1 \right) \right\}. \tag{18}$$

During the competitive period, the preselected vehicle needs to wait for an Arbitration Inter Frame Space (AIFS) after the channel detection is idle. The representation of AIFS is shown in (11).

For different priorities of data, the values set for SIFS are the same, and the values set for AIFSN are not the same. Thus, according to Formula (11), different AIFS can be obtained by setting different values of AIFSN. After waiting for an AIFS, the eligible vehicle turns on the back-off timer, and the back-off time is expressed as

$$T = CW \times \operatorname{Random}(0,1) \times \operatorname{slotTime}, \tag{19}$$

where the initial value of CW is set to CW_{\min} , and the value of CW increases as $(CW + 1) \times 2 - 1$ for each collision, and remains constant when added to CW_{\max} . After the data transfer is completed, it returns to the initial value CW_{\min} . Combined with Formula (11) and Formula (19), the total time that the eligible vehicle in the competitive phase needs to wait is expressed as

$$t = AIFS + T = SIFS + AIFSN \times \operatorname{slotTime} + CW \times \operatorname{Random}(0,1) \times \operatorname{SlotTime}. \tag{20}$$

After an AIFS, the preselected vehicles compete with each other, and only the one which has the minimum timer is selected as the active node and allowed to transmit.

As Q_q is obtained, the density of the point process formed by the eligible transmitters is given by $\lambda_q = \lambda_t Q_q$, and Φ_q denotes the point process formed by the eligible transmitters. Consider two

arbitrary eligible transmitters X and $Z_i(X, Z_i \in \Phi_q)$, we define Z_i as the contender of X , only if $PH|Z_i - X|^{-\alpha} \geq \theta_q$, where θ_q is the predefined carrier sensing threshold in the contention period. Thus, the density of the contenders around X is computed as $\lambda_c = \lambda_q \Pr\left(\frac{PH}{r^\alpha} \geq \theta_q\right) = \lambda_t Q_q \exp\left(-\frac{\theta_q r^\alpha}{P}\right)$. We assume Π_c^X is the set of all the contenders around X , and m_i is the total waiting timer of the contender Z_i . Then, the probability that the preselected vehicle is ultimately allowed to transmit is derived as

$$Q_c = E \left[\prod_{Z_i \in \Pi_c^X} \Pr(m_i \geq t) \right] = E_t \left[\exp \left(-2 \int_0^\infty (1 - \Pr(m_Y \geq t)) \lambda_c dr \right) \right]. \tag{21}$$

In VANET, the application messages are divided into four access categories according to the delay sensitivity. We assume that the probability of occurrence of different priority services is the same as 1/4. Since the calculation process is similar, we only analyze the transmission opportunities for the highest priority message. In Formula (21), the value of SIFS is fixed, so we simplify the total waiting time t in the contention phase to $t' = AIFSN + CW \times Random(0, 1)$. Set $AIFSN_i$ and CW_i as the priority of arbitration inter frame space and contention window.

For the highest priority message ($t' \in [AIFSN_1, AIFSN_1 + CW_1]$), we have

$$\begin{aligned} \Pr(m_i \geq t') &= 1 - \Pr(m_i < t') \\ &= \begin{cases} 1 - \left\{ P_{P1} \int_{AIFSN_1}^{t'} \frac{1}{CW_1} dt + (1 - P_{P1}) \int_{AIFSN_i}^{t'} \frac{1}{CW_i} dt \right\}, & t' \geq AIFSN_i \\ 1 - \left\{ P_{P1} \int_{AIFSN_1}^{t'} \frac{1}{CW_1} dt \right\}, & AIFSN_1 \leq t' < AIFSN_i \\ 1 - \left(\frac{P_{P1}(t' - AIFSN_1)}{CW_1} + \frac{(1 - P_{P1})(t' - AIFSN_i)}{CW_i} \right), & t' \geq AIFSN_i \\ 1 - \left(\frac{P_{P1}(t' - AIFSN_1)}{CW_1} \right), & AIFSN_1 \leq t' < AIFSN_i \end{cases} \end{aligned} \tag{22}$$

Then, under the highest priority, Q_c^h is calculated as

$$\begin{aligned} Q_c^h &= E_{t'} \left[\exp \left(-2 \int_0^\infty (1 - \Pr(m_i \geq t')) \lambda_c dr \right) \right] = \int_{AIFSN_1}^{AIFSN_i} \frac{1}{CW_1} \exp \left[-2 \left(\frac{P_{P1}(t' - AIFSN_1)}{CW_1} \right) \int_0^\infty \lambda_t Q_q e^{-\frac{\theta_q r^\alpha}{P}} dr \right] dt' \\ &+ \int_{AIFSN_i}^{AIFSN_1 + CW_1} \frac{1}{CW_1} \exp \left[-2 \left(\frac{P_{P1}(t' - AIFSN_1)}{CW_1} + \frac{(1 - P_{P1})(t' - AIFSN_i)}{CW_i} \right) \int_0^\infty \lambda_t Q_q e^{-\frac{\theta_q r^\alpha}{P}} dr \right] dt' \end{aligned} \tag{23}$$

For the lowest priority message ($t' \in [AIFSN_8, AIFSN_8 + CW_8]$), we have

$$\begin{aligned} \Pr(m_i \geq t') &= 1 - \Pr(m_i < t') \\ &= \begin{cases} 1 - \left\{ P_{P8} \int_{AIFSN_8}^{t'} \frac{1}{CW_8} dt + (1 - P_{P8}) \int_{AIFSN_i}^{t'} \frac{1}{CW_i} dt \right\}, & t' \leq CW_i + AIFSN_i \\ 1 - \left\{ P_{P8} \int_{AIFSN_8}^{t'} \frac{1}{CW_8} dt + (1 - P_{P8}) \right\}, & CW_8 + AIFSN_8 \geq t' > CW_i + AIFSN_i \\ 1 - \left\{ \frac{P_{P8}(t' - AIFSN_8)}{CW_8} + \frac{(1 - P_{P8})(t' - AIFSN_i)}{CW_i} \right\}, & t' \leq CW_i + AIFSN_i \\ 1 - \left\{ \frac{P_{P8}(t' - AIFSN_8)}{CW_8} + (1 - P_{P8}) \right\}, & CW_8 + AIFSN_8 \geq t' > CW_i + AIFSN_i \end{cases} \end{aligned} \tag{24}$$

Then, under the lowest priority, Q_c^l is calculated as

$$\begin{aligned} Q_c^l &= E_{t'} \left[\exp \left(-2 \int_0^\infty (1 - \Pr(m_i' \geq t')) \lambda_i^c dr \right) \right] \\ &= \int_{AIFSN_8}^{AIFSN_i + CW_i} \frac{1}{CW_8} \exp \left[-2 \left(\frac{P_{P8}(t' - AIFSN_8)}{CW_8} + \frac{(1 - P_{P8})(t' - AIFSN_i)}{CW_i} \right) \int_0^\infty \lambda_t Q_q e^{-\frac{\theta_q r^\alpha}{P}} dr \right] dt' \\ &+ \int_{AIFSN_i + CW_i}^{AIFSN_8 + CW_8} \frac{1}{CW_1} \exp \left[-2 \left(\frac{P_{P8}(t' - AIFSN_8)}{CW_8} + (1 - P_{P8}) \right) \int_0^\infty \lambda_t Q_q e^{-\frac{\theta_q r^\alpha}{P}} dr \right] dt' \end{aligned} \tag{25}$$

Lemma 2. When Q_q and Q_c are derived as above, the transmission opportunity of an arbitrary vehicle under the EDCA protocol is thereby characterized as $Q = Q_q Q_c$.

4.2. Transmission Opportunity Under CSMA/CA

The CSMA/CA can also be modeled as a two-phase protocol for theoretical analysis. Let \tilde{Q}_q be the probability that a vehicle is selected as a preselected transmitter during the sensing period in CSMA/CA, and \tilde{Q}_c be the probability that the preselected vehicle is ultimately allowed to transmit.

In the sensing period, the calculation of \tilde{Q}_q is the same as Q_q , that is $\tilde{Q}_q = Q_q$. In the competitive period, the preselected vehicle is allowed to transmitter only if its back-off time is the smallest among the other contenders. Different from EDCA, all data-packets under CSMA/CA are assumed to hold the same priority. Therefore, \tilde{Q}_c is calculated as

$$\begin{aligned} \tilde{Q}_c &= E \left[\prod_{Z_i \in \Pi_c^X} \Pr(m_i \geq t) \right] \\ &= \int_0^{CW} \frac{1}{CW} \exp \left(-2 \frac{t}{CW} \int_0^\infty \lambda_t Q_q e^{-\frac{\theta_{cr} r^\alpha}{P}} dr \right) dt = \frac{1 - e^{-\left(\frac{2\lambda_t Q_q}{\alpha} \left(\frac{\theta_c}{P_s} \right)^{-\frac{1}{\alpha}} \Gamma\left(\frac{1}{\alpha}\right) \right)}}{\frac{2\lambda_t Q_q}{\alpha} \left(\frac{\theta_c}{P_s} \right)^{-\frac{1}{\alpha}} \Gamma\left(\frac{1}{\alpha}\right)} \end{aligned} \tag{26}$$

From Formula (24), Formula (26), and Formula (27), we can prove that

$$\begin{aligned} Q_c^h &> \int_{AIFSN_1}^{AIFSN_1 + CW_1} \frac{1}{CW_1} \exp \left[-2 \left(\frac{P_{P1}(t' - AIFSN_1)}{CW_1} + \frac{(1 - P_{P1})(t' - AIFSN_1)}{CW_1} \right) \int_0^\infty \lambda_t Q_q e^{-\frac{\theta_{cr} r^\alpha}{P}} dr \right] dt' \\ &= \int_0^{CW_1} \frac{1}{CW_1} \exp \left[-2 \frac{t'}{CW_1} \int_0^\infty \lambda_t Q_q e^{-\frac{\theta_{cr} r^\alpha}{P}} dr \right] dt' = \tilde{Q}_c \end{aligned} \tag{27}$$

$$\begin{aligned} Q_c^l &< \int_{AIFSN_8}^{AIFSN_8 + CW_8} \frac{1}{CW_8} \exp \left[-2 \left(\frac{P_{P8}(t' - AIFSN_8)}{CW_8} + \frac{(1 - P_{P8})(t' - AIFSN_8)}{CW_8} \right) \int_0^\infty \lambda_t Q_q e^{-\frac{\theta_{cr} r^\alpha}{P}} dr \right] dt' \\ &= \int_0^{CW_8} \frac{1}{CW_8} \exp \left[-2 \frac{t'}{CW_8} \int_0^\infty \lambda_t Q_q e^{-\frac{\theta_{cr} r^\alpha}{P}} dr \right] dt' = \tilde{Q}_c \end{aligned} \tag{28}$$

4.3. Outage Probability

Because of the complexity of the distribution of the nodes in VANET, it is difficult to calculate the statistical distribution of all the interference nodes in the network. According to the bound effect of interference power in the wireless network, the first layer of interferers can only be considered instead of the aggregated simultaneous transmitters [25].

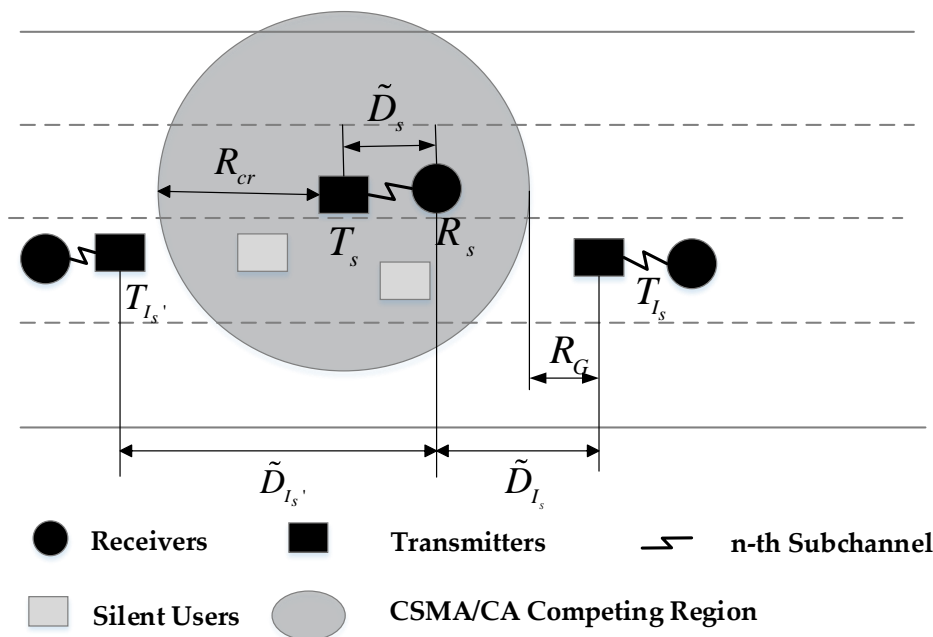


Figure 4. Interfered scenario.

As shown in Figure 4, the worst interfered case is considered where the vehicles transmitting concurrently are just outside the competition region (CR). Assume the reference receiver R_0 locate at the origin, and its corresponding transmitter is denoted by T_0 , and the distance between T_0 and R_0 is expressed as D_s . Denote the right and left interfering nodes of R_0 as T_1 and T_2 , and the distances between T_1 and R_0 , T_2 and R_0 are expressed as D_{I_1} and D_{I_2} , respectively. Since the boundary of CR uniformly locates between two adjacent vehicle nodes, the distance between the right boundary of T_0 's CR and T_1 is expressed as $R_G = X \cdot U$, where X is the distance between any two adjacent vehicle nodes, and U is uniformly distributed within $[0,1]$. Therefore, the cumulative distribution function (CDF) and probability density function (PDF) of R_G can be calculated as

$$F_{R_G}(y) = \Pr\{X \cdot U \leq y\} = \int_0^\infty \Pr\{U \leq \frac{y}{x}\} \cdot f_X(x) dx$$

$$= y \cdot \exp\left(\frac{\sigma^2}{2} - \mu\right) \cdot \Phi\left(\frac{\mu - \sigma^2 - Iny}{\sigma}\right) + \Phi\left(\frac{Iny - \mu}{\sigma}\right) \tag{29}$$

$$f_{R_G}(y) = \frac{dF_{R_G}(y)}{dy} = \int_0^\infty \left[\exp\left(\frac{\sigma^2}{2} - \mu\right) \cdot \Phi\left(\frac{\mu - \sigma^2 - Iny}{\sigma}\right) - \frac{1}{\sqrt{2\pi}} \exp\left(\frac{\sigma^2}{2} - \mu - \frac{(\mu - \sigma - Iny)^2}{2\sigma^2}\right) + \frac{1}{\sqrt{2\pi\sigma y}} \exp\left(-\frac{(Iny - \mu)^2}{2\sigma^2}\right) \right] dx \tag{30}$$

Duo to the symmetry feature, D_2 has the identical PDF of D_1 . Given $D_s = d_s$, the conditional PDF of D_1 and D_2 is derived, respectively, as follow

$$f_{D_{I_1}/d_s}(d) = f_{R_G}(d - R_{cr} + d_s), \tag{31}$$

$$f_{D_{I_2}/d_s}(d) = f_{R_G}(d + R_{cr} + d_s). \tag{32}$$

According to Formula (4), the outage probability τ is derived as follows

$$\tau = \Pr(SIR \leq \beta) = P\left(\frac{PHd_s}{P_{I_1} + P_{I_2}} \leq \beta\right) = P(H \leq \beta d_s (I_1 + I_2))$$

$$= 1 - E[\exp(-\beta d_s^\alpha I_1)] E[\exp(-\beta d_s^\alpha I_2)], \tag{33}$$

where $I_1 = HD_{I_1}$, and $I_2 = HD_{I_2}$ denote the interference experiences by R_0 from T_1 and T_2 respectively.

$$E[\exp(-\beta d_s^\alpha I_1)] = E\left[\exp\left(-\beta d_s^\alpha HD_{I_1}^{-\alpha}\right)\right] = \int_0^\infty f_{D_{I_1}}(x) E_H[\exp(-\beta d_s^\alpha Hx^{-\alpha})] dx$$

$$= \int_0^\infty \left[\exp\left(\frac{\sigma^2}{2} - \mu\right) \cdot \Phi\left(\frac{\mu - \sigma^2 - In(x - R_{cr} + d_s)}{\sigma}\right) - \frac{1}{\sqrt{2\pi}} \exp\left(\frac{\sigma^2}{2} - \mu - \frac{(\mu - \sigma - In(x - R_{cr} + d_s))^2}{2\sigma^2}\right) + \frac{\exp\left(-\frac{(In(x - R_{cr} + d_s) - \mu)^2}{2\sigma^2}\right)}{\sqrt{2\pi\sigma(x - R_{cr} + d_s)}} \right] \frac{dx}{\beta d_s^\alpha x^{-\alpha} + 1} \tag{34}$$

$$E[\exp(-\beta d_s^\alpha I_2)] = E\left[\exp\left(-\beta d_s^\alpha HD_{I_2}^{-\alpha}\right)\right]$$

$$= \int_0^\infty \left[\exp\left(\frac{\sigma^2}{2} - \mu\right) \cdot \Phi\left(\frac{\mu - \sigma^2 - In(x + R_{cr} + d_s)}{\sigma}\right) - \frac{1}{\sqrt{2\pi}} \exp\left(\frac{\sigma^2}{2} - \mu - \frac{(\mu - \sigma - In(x + R_{cr} + d_s))^2}{2\sigma^2}\right) + \frac{\exp\left(-\frac{(In(x + R_{cr} + d_s) - \mu)^2}{2\sigma^2}\right)}{\sqrt{2\pi\sigma(x + R_{cr} + d_s)}} \right] \frac{dx}{\beta d_s^\alpha x^{-\alpha} + 1} \tag{35}$$

Lemma 3. When the transmission opportunity Q and the outage probability τ are derived, the transmission capacity $C_T = \lambda_t Q(1 - \tau)$ of the linear VANET under the EDCA protocol is thereby characterized.

5. Simulation Results

We build a 1-dimensional linear VANET environment with Matlab to validate the theoretical results. Under the long enough straight road environment, the whole EDCA channel access mechanism

is simulated (the parameters take the values specified in 802.11p), and the channels are Rayleigh fading and path-loss fading. Each vehicle transmits frames with a constant bit rate and the moving pattern is described as classic car-following model. In addition, we present some numerical analytical results, such as the relationship between transmission opportunity and maximum received beacon power threshold and predefined carrier sensing threshold. The parameters are shown in Table 3.

Table 3. Simulation parameters.

Simulation Parameter	Numerical Value	Simulation Parameter	Numerical Value
IEEE 802.11std	802.11p	Transmission Gain G_t	34 dBm
CCA mode	CCA mode 1	Receiving Gain G_r	33 dBm
Carrier Wavelength λ	0.051 m	CCA Threshold θ_c	-75 dBm
Packet Length	2048 byte	Exponent α	2
Slot-time	20 μ s	Outage Probability τ	0
[CW_{\min} , CW_{\max}]	[140 μ s, 300 μ s]	Transmission Data-rate R	2 Mbps
Arbitration Inter-Frame Space (AIFS)	50 μ s	Effective Transmission Radium D	500 m
Short Inter-frame Space (SIFS)	10 μ s	Road Length L	4 km
Transmission Power P_t	33 dBm	Duration of Simulation t_s	3 s

The simulation results on transmission opportunity and capacity with highest and lowest priority under EDCA versus the density of vehicles are illustrated and compared with those without priority under CSMA/CA in Figures 5 and 6, respectively, where $\theta_c = -75$ dBm. In Figure 5, it can be observed that the transmission opportunity is a decreasing function of the density of vehicles. This is because that, with the increase of potential transmitters, the completion that the reference vehicle is confronted with becomes more intense. It can also be observed that the vehicles with highest priority under EDCA has more transmission opportunity than the vehicles without priority under CSMA/CA. This can be attributed to the reason that the vehicles with highest priority under EDCA have shorter back-off time in comparison to the vehicles with the lowest priority in the contention period. In Figure 6, the simulation results show that the network transmission capacity increases slowly as vehicle density increases. This is because in low density scenes, the number of active transmitters in the whole network increases with the increase of vehicle density, and the network transmission capacity also increases. On the other hand, more vehicles competing for access to the channel will lead to more collision and transmission outage. In the end, the transmission capacity tends to be flat. Figure 6 also shows that the network transmission capacity is improved obviously under the EDCA with the highest priority. The results in both figures are consistent with the theoretical analysis results in Formula (27), Formula (28) and Lemma 3.

Figure 7 gives the simulation results of the transmission capacity versus the transmission opportunity with highest priority under EDCA, where $\lambda = 10, 15/\text{km}$, respectively. It is notable that the transmission capacity increases when the transmission opportunity increases. This shows that for the design of the MAC protocol, the focus of improving network transmission capacity is to design a high transmission opportunity that can avoid information collision with limited interference. It also proves that the simulation results are consistent with the theoretical results.

The analytical results on transmission opportunity with highest priority under EDCA versus maximum received beacon power threshold θ_c are shown in Figure 8, where $\lambda = 50, 10/\text{km}$ respectively, and $\theta_q = -75$ dBm. It is evident from the results that the transmission opportunity is an increasing function of θ_c , and it decreases as the density of transmitter increases. This can be attributed to the reason that the probability that potential transmitters become alternate transmitters increases with the increases of θ_c , therefore, the transmission opportunity also increases. On the other

hand, with the decrease of λ , the competition for alternative transmitters in the contention period decreases, and the network transmission opportunity increases. Figure 9 shows the transmission opportunity with the highest priority under EDCA versus the predefined carrier sensing threshold θ_q , where $\lambda = 50, 10/\text{km}$, respectively, and $\theta_c = -75 \text{ dBm}$. It is evident from the results that the network transmission opportunity is an increasing function of θ_q , and it increases as the density of the transmitter decreases. This is because, with the increase of the competition threshold θ_q , the density of transmitters which competing with the alternate transmitter becomes smaller, thus the probability of alternative transmitters competing for success increases. Compared with Figure 8, the transmission opportunity has a closer relationship to λ in Figure 9.

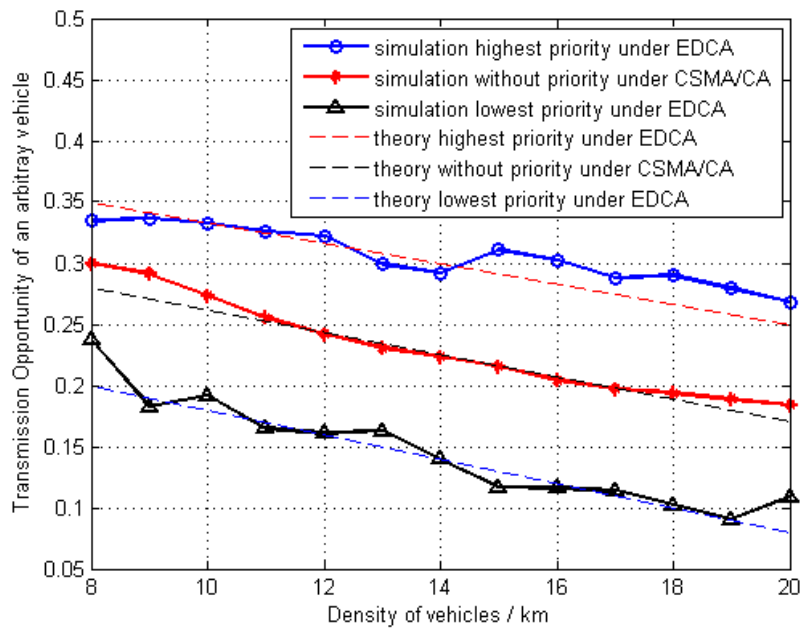


Figure 5. Transmission opportunity with different priorities versus the density of the active transmitters.

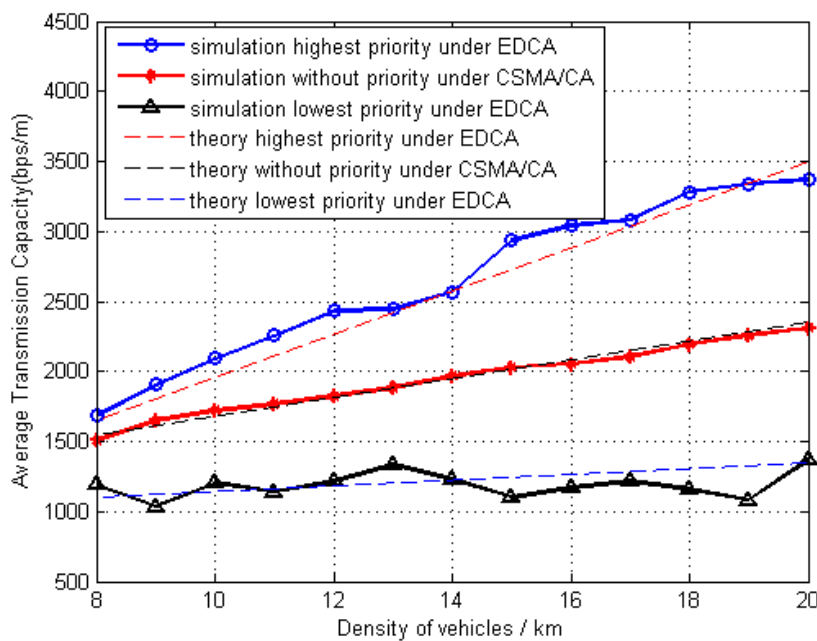


Figure 6. Transmission capacity with different priorities versus the density of the active transmitters.

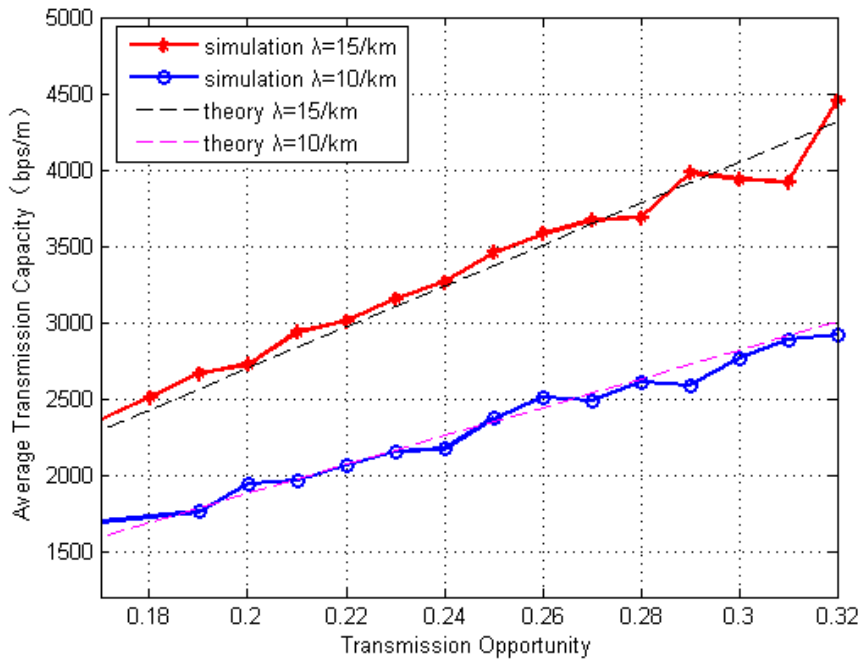


Figure 7. Average transmission capacity with highest priority versus transmission opportunity.

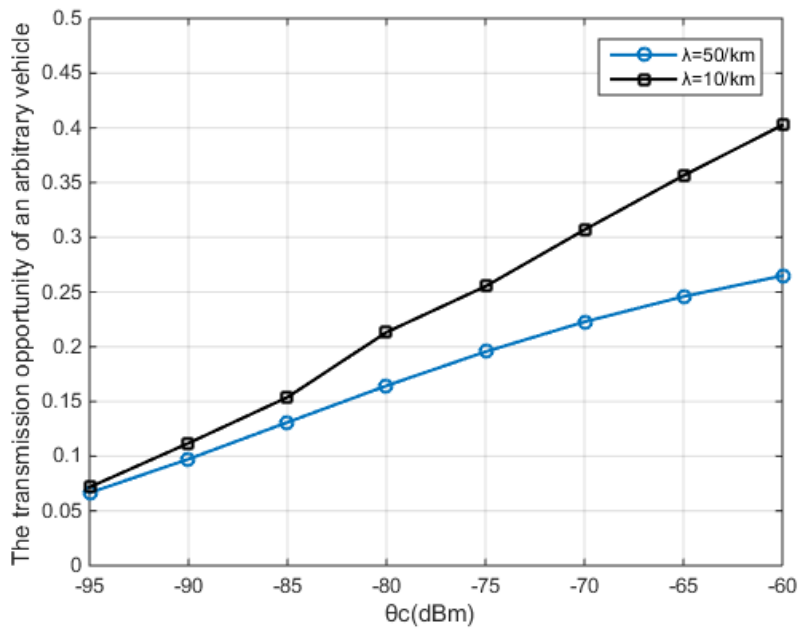


Figure 8. The transmission opportunity with highest priority versus maximum received beacon power threshold.

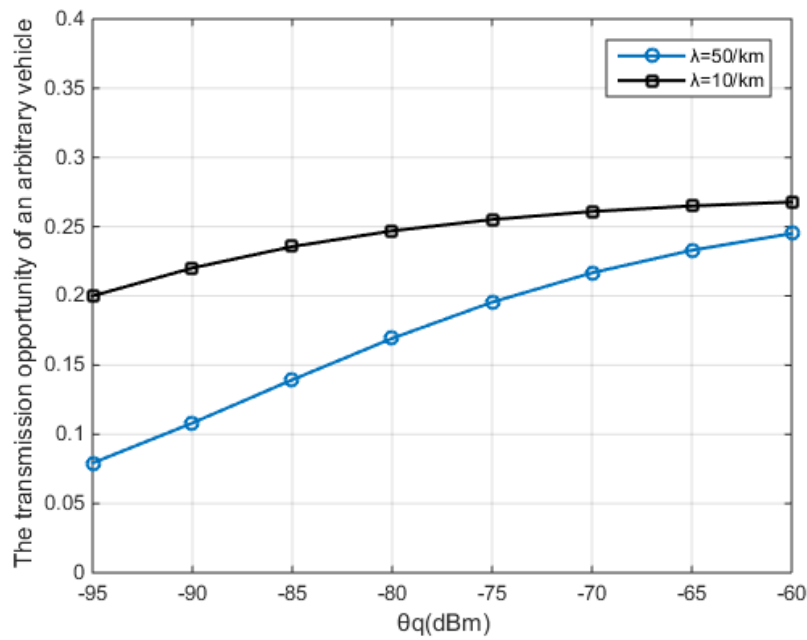


Figure 9. The transmission opportunity with highest priority versus predefined carrier sensing threshold.

From Figure 10, the relationship between outage probability and SIR threshold is illustrated, where $d_s = 150, 200$ m respectively. The outage probability logarithmically increase while SIR threshold increases and approach to 1 when β larger than 1000. The higher SIR Threshold means a higher QoS requirement. The outage probability also increases when the value of d_s increases, as the reason of the signal received at the receiver from the reference transmitters is decreased, and the SIR is thereby decreased.

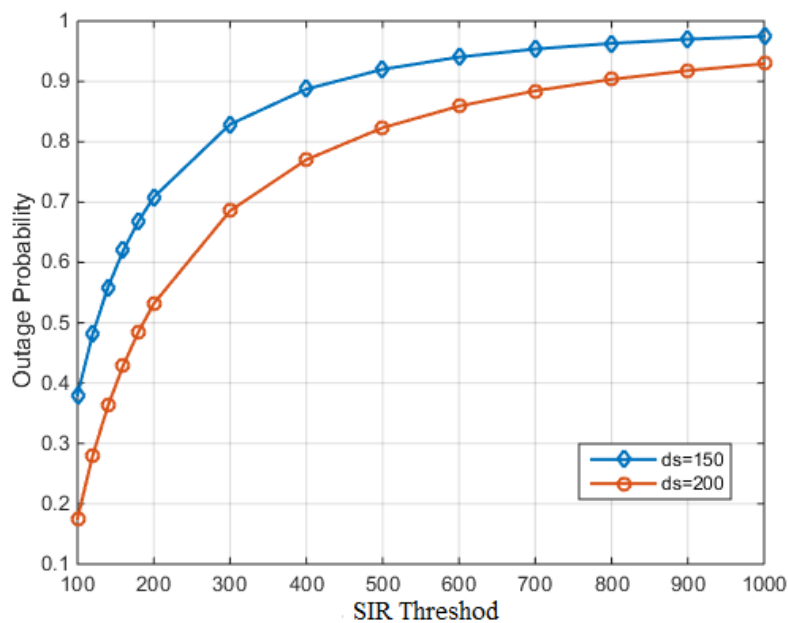


Figure 10. Outage probability versus SIR threshold β .

6. Conclusions

In this paper, the transmission capacity under EDCA in VANETs environment is analyzed from the perspective of the spatial geometric relationship among transmitters. In our study, the transmission scheme is set to mimic EDCA protocol, and the moving pattern of vehicles is described as the

classic car-following model based on lognormal distribution. Based on this model, the transmission opportunity and the outage probability under EDCA protocol are calculated by applying tools from stochastic geometry, and the transmission capacity of 1-dimensional VANET is thereby obtained. Finally, the highest priority and lowest priority of transmission opportunities and transmission capacity under this model are simulated, the theoretical results are verified, and the change rules of transmission opportunity and outage probability with the specific parameters are more intuitive. In the future, the convergence of wireless network and optical network can improve network performance such as large bandwidth, high speed, and low latency [30]. Some scholars have proposed to use optical wireless communication to improve the performance of vehicular communication [31], which is also our next research focus.

Author Contributions: Investigation, W.L. and X.H.; Software, W.L. and X.H.; Methodology, X.H.; Visualization, W.L.; Writing: original draft, W.L.; Writing: review and editing, X.H., Z.H. and Y.J.; Supervision, Z.H. and Y.J.; Project administration, Z.H.; Funding acquisition, Z.H. and Y.J.

Funding: This work was supported in part by National Key R&D Program of China (No.2017Y FB0403605), and National Natural Science Foundation of China (No.61801165).

Conflicts of Interest: The authors declare no conflict of interest.

References

1. Sheet, D.K.; Kaiwartya, O.; Abdullah, A.H.; Cao, Y.; Hassan, N.S.; Kumar, S. Location information verification using transferable belief model for geographic routing in vehicular ad hoc networks. *IET Intell. Transp. Syst.* **2017**, *11*, 53–60. [[CrossRef](#)]
2. Kaiwartya, O.; Abdullah, A.H.; Cao, Y.; Altameem, A.; Prasad, M.; Lin, C.T.; Liu, X. Internet of vehicles: Motivation, layered architecture, network model, challenges, and future aspects. *IEEE Access* **2016**, *4*, 5356–5373. [[CrossRef](#)]
3. Qureshi, K.N.; Abdullah, A.H.; Kaiwartya, O.; Iqbal, S.; Butt, R.A.; Bashir, F. A dynamic congestion control scheme for safety applications in vehicular ad hoc networks. *Comput. Electr. Eng.* **2018**, *72*, 774–788. [[CrossRef](#)]
4. Aliyu, A.; Abdullah, H.; Kaiwartya, O.; Cao, Y.; Usman, M.J.; Kumar, S.; Lobiyal, D.K.; Raw, R.S. Cloud computing in VANETs architecture, taxonomy, and challenges. *IETE Tech. Rev.* **2018**, *35*, 523–547. [[CrossRef](#)]
5. Xia, Y.; Chen, W.; Liu, X.; Zhang, L.; Li, X.; Xiang, Y. Adaptive multimedia data forwarding for privacy preservation in Vehicular Ad-Hoc Networks. *IEEE Trans. Intell. Transp.* **2017**, *18*, 2629–2641. [[CrossRef](#)]
6. Gupta, P.; Kumar, P.R. The capacity of wireless networks. *IEEE Trans. Inf. Theory* **2000**, *46*, 388–404. [[CrossRef](#)]
7. Baccelli, F.; Blaszczyzyn, B.; Muhlethaler, P. An Aloha protocol for multihop mobile wireless networks. *IEEE Trans. Inf. Theory* **2006**, *2*, 421–436. [[CrossRef](#)]
8. Weber, S.; Andrews, J.G.; Jindal, N. The effect of fading, channel inversion, and threshold scheduling on ad hoc networks. *IEEE Trans. Inf. Theory* **2007**, *11*, 4127–4149. [[CrossRef](#)]
9. Baccelli, F.; Blaszczyzyn, B. Stochastic Geometry and Wireless Networks. *NOW Found. Trends Netw.* **2010**, *4*, 1–312.
10. Haenggi, M.; Andrews, J.G.; Baccelli, F.; Dousse, O.; Franceschetti, M. Stochastic geometry and random graphs for the analysis and design of wireless networks. *IEEE J. Sel. Areas Commun.* **2009**, *7*, 1029–1046. [[CrossRef](#)]
11. Weber, S.; Andrews, J.G. Transmission capacity of wireless networks. *Found. Trends Netw.* **2012**, *5*, 3593–3604. [[CrossRef](#)]
12. Kasana, R.; Kumar, S.; Kaiwartya, O.; Kharel, R.; Lloret, J.; Aslam, N.; Wang, T. Fuzzy-based channel selection for location oriented services in multichannel VCPS environments. *IEEE Internet Things* **2018**, *5*, 4642–4651. [[CrossRef](#)]
13. Hassan, A.N.; Kaiwartya, O.; Abdullah, A.H.; Sheet, D.H.; Raw, R.S. Inter-vehicle distance based connectivity aware routing in vehicular adhoc networks. *Wirel. Pers. Commun.* **2018**, *98*, 33–54. [[CrossRef](#)]
14. Lu, N.; Luan, T.H.; Wang, M.; Shen, X.; Bai, F. Capacity and delay analysis for social-proximity urban vehicular networks. In Proceedings of the IEEE INFOCOM, Orlando, FL, USA, 25–30 March 2012; pp. 1476–1484.

15. Huang, Y.; Chen, M.; Cai, Z.; Guan, X.; Ohtsuki, T.; Zhang, Y. Graph Theory Based Capacity Analysis for Vehicular Ad Hoc Networks. In Proceedings of the 2015 IEEE Global Communications Conference, San Diego, CA, USA, 6–10 December 2015. [[CrossRef](#)]
16. Wang, M.; Shan, H.; Luan, T.H.; Lu, N.; Zhang, R.; Shen, X.; Bai, F. Asymptotic Throughput Capacity Analysis of VANETs Exploiting Mobility Diversity. *IEEE Trans. Veh. Technol.* **2015**, *64*, 4187–4202. [[CrossRef](#)]
17. Jacquet, P.; Muhlethaler, P. Mean Number of Transmissions with CSMA in a Linear Network. In Proceedings of the Vehicular Technology Conference, Ottawa, ON, Canada, 6–9 September 2010. [[CrossRef](#)]
18. Giang, A.T.; Busson, A.; Lambert, A.; Gruyer, D. An upper bound for capacity of VANET. In Proceedings of the 2012 International Conference on Advanced Technologies for Communications, Hanoi, Vietnam, 10–12 October 2012. [[CrossRef](#)]
19. Ozturk, S.; Mi, J.; Mi, V.B. Capacity limits in a variable duty cycle IEEE 802.11p-based VANET. *Wirel. Commun. Mob. Comput.* **2012**, *12*, 1672–1684. [[CrossRef](#)]
20. Giang, A.T.; Busson, A.; Gruyer, D.; Lambert, A. A packing model to estimate VANET capacity. In Proceedings of the Wireless Communications and Mobile Computing Conference (IWCMC), Limassol, Cyprus, 27–31 August 2012; pp. 1119–1124.
21. Ni, M.; Pan, J.; Cai, L.; Yu, J.; Wu, H.; Zhong, Z. Interference-Based Capacity Analysis for Vehicular Ad Hoc Networks. *IEEE Commun. Lett.* **2015**, *19*, 621–624. [[CrossRef](#)]
22. Donadee, J.; Marija, D. Stochastic Optimization of Grid to Vehicle Frequency Regulation Capacity Bids. *IEEE Trans. Smart Grid* **2014**, *5*, 1061–1069. [[CrossRef](#)]
23. Luan, T.H.; Ling, X.; Shen, X. MAC in Motion: Impact of Mobility on the MAC of Drive-Thru Internet. *IEEE Trans. Mob. Comput.* **2011**, *11*, 305–319. [[CrossRef](#)]
24. He, X.; Shi, W.; Luo, T. Transmission Capacity Analysis for Vehicular Ad Hoc Networks. *IEEE Access* **2018**, *6*, 30333–30341. [[CrossRef](#)]
25. Le, D.T. A Priority-Based Multichannel Mac to Support the Non-Safety Applications in SCH Interval at RSU in V2I Communication. *Transp. Telecommun. J.* **2018**, *19*, 269–283. [[CrossRef](#)]
26. Brackstone, M.; McDonald, M. Car-following: A historical review. *Transportation Research Part F. Traffic Psychol. Behav.* **1999**, *2*, 181–196. [[CrossRef](#)]
27. Shiraki, Y.; Ohyama, T.; Nakabayashi, S. Development of an Inter-Vehicle communications system. *IEEE Trans. Intell. Transp. Syst.* **2001**, *68*, 11–13.
28. Lu, N.; Zhang, N.; Cheng, N.; Shen, X. Vehicles meet infrastructure: Toward capacity cost tradeoffs for vehicular access networks. *IEEE Trans. Intell. Transp. Syst.* **2013**, *14*, 1266–1277. [[CrossRef](#)]
29. Ni, M.; Zhang, L.; Pan, J.; Cai, L.; Rutagemwa, H.; Li, L.; Wei, T. Connectivity in mobile tactical networks. In Proceedings of the 2014 IEEE Global Communications Conference, Austin, TX, USA, 8–12 December 2014; pp. 4400–4405.
30. Ji, Y.; Zhang, J.; Wang, X.; Yu, H. Towards converged, collaborative and co-automatic (3C) optical networks. *Sci. China Inf. Sci.* **2018**, *61*, 121301. [[CrossRef](#)]
31. Ucar, S.; Ergen, S.C.; Ozkasap, O. IEEE 802.11p and Visible Light Hybrid Communication based Secure Autonomous Platoon. *IEEE Trans. Veh. Technol.* **2018**, *67*, 8667–8681. [[CrossRef](#)]

